

INFRARED SPECTROSCOPY OF DUST IN THE DIFFUSE INTERSTELLAR MEDIUM TOWARD CYGNUS OB2 NO. 12¹

D. C. B. WHITTET,² A. C. A. BOOGERT,³ P. A. GERAKINES,² W. SCHUTTE,⁴ A. G. G. M. TIELENS,^{3,5}
TH. DE GRAAUW,^{3,6} T. PRUSTI,⁷ E. F. VAN DISHOECK,⁴
P. R. WESSELIUS,⁶ AND C. M. WRIGHT^{4,8}

Received 1997 April 17; accepted 1997 July 11

ABSTRACT

Observations made with the short-wavelength spectrometer of the *Infrared Space Observatory* are used to investigate the composition of interstellar dust in the line of sight to Cygnus OB2 No. 12, commonly taken as representative of the diffuse (low-density) interstellar medium. Results are compared with data for the Galactic center source Sgr A*. Nondetections of the 3.0 and 4.27 μm features of H₂O and CO₂ ices in Cyg OB2 No. 12 confirm the absence of dense molecular material in this line of sight, whereas the presence of these features in Sgr A* indicates that molecular clouds may contribute as much as 10 mag of visual extinction toward the Galactic center. The spectrum of Cyg OB2 No. 12 is dominated by the well-known 9.7 μm silicate feature; detection of a shallow feature near 2.75 μm indicates that the silicates are at least partially hydrated, with composition possibly similar to that of terrestrial phyllosilicates such as serpentine or chlorite. However, the 2.75 μm feature is not seen in the Galactic center spectrum, suggesting that silicates in this line of sight are less hydrated or of different composition. The primary spectral signatures of C-rich dust in the diffuse ISM are weak absorptions at 3.4 μm (the aliphatic C—H stretch) and 6.2 μm (the aromatic C=C stretch). We conclude, based on infrared spectroscopy, that the most probable composition of the dust toward Cyg OB2 No. 12 is a mixture of silicates and carbonaceous solids in a volume ratio of approximately 3:2, with the carbonaceous component primarily in an aromatic form such as amorphous carbon.

Subject headings: dust, extinction — Galaxy: center — infrared: ISM: lines and bands —
ISM: abundances — ISM: molecules — stars: individual (Cyg OB2 No. 12)

1. INTRODUCTION

The composition of dust in the diffuse ISM is a long-term problem in astrophysics.⁹ Interstellar extinction has been well studied in such regions within a few kpc of the Sun (see, e.g., Mathis 1990). There is general agreement that the dust responsible for extinction must include both carbon-rich and oxygen-rich materials, and that both circumstellar and interstellar sources of dust are required to explain the total opacity per H atom (Jones et al. 1994). However, the nature of the dust remains controversial, owing largely to the lack of uniqueness in existing models of extinction. New constraints on the abundances and depletions of heavy elements available to form grains in the ISM present a severe challenge to these models (Mathis 1996).

Infrared spectroscopy provides a potentially powerful and direct technique for investigating grain composition.

¹ Based on observations with *ISO*, a European Space Agency (ESA) project, with instruments funded by ESA Member States (especially the P.I. countries France, Germany, the Netherlands, and the United Kingdom) and with the participation of ISAS and NASA.

² Department of Physics, Applied Physics, and Astronomy, Rensselaer Polytechnic Institute, Troy, NY 12180.

³ Kapteyn Astronomical Institute, P.O. Box 800, 9700 AV Groningen, The Netherlands.

⁴ Leiden Observatory, P.O. Box 9513, 2300 RA Leiden, The Netherlands.

⁵ NASA Ames Research Center, Mail Stop 245-6, Moffet Field, CA 94035.

⁶ SRON, P.O. Box 800, 9700 AV Groningen, The Netherlands.

⁷ *ISO* Science Operations Center, Astrophysics Division, ESA, Villafranca del Castillo, P.O. Box 50727, 28080 Madrid, Spain.

⁸ Max-Planck-Institut für extraterrestrische Physik, Postfach 1603, D-85740 Garching, Germany.

⁹ “Diffuse ISM” is here taken to mean low-density ($n \lesssim 100 \text{ cm}^{-3}$) phases of the ISM outside of dense molecular clouds, encompassing the intercloud medium and diffuse clouds.

Previous observations from ground-based and airborne telescopes have advanced our understanding considerably. The broad feature centered at 9.7 μm , observed in many lines of sight, is identified with Si—O bonds in amorphous silicates (Gillett et al. 1975; Roche & Aitken 1984). The absence of a corresponding feature at 11.2 μm arising in silicon carbide indicates that Si is almost exclusively tied up in oxygen-rich dust in the diffuse ISM (Whittet, Duley, & Martin 1990). Carbon-rich dust has been identified by means of absorptions at 3.4 and 6.8 μm , attributed to CH₂ and CH₃ groups in saturated aliphatic hydrocarbons (Sandford et al. 1991; Pendleton et al. 1994; Tielens et al. 1996), but as much as one-third of the grain mass may yet be unaccounted for (Tielens et al. 1996). With the availability of data from the *Infrared Space Observatory* (*ISO*) we now have the opportunity to obtain complete spectral coverage of the infrared vibrational spectrum of interstellar dust.

Our ability to sample the diffuse ISM adequately is limited by the availability of background sources with high extinctions arising outside of molecular clouds. One of the best studied lines of sight is that to the highly reddened B-type hypergiant star Cygnus OB2 No. 12.¹⁰ We present here the first *ISO* observations of this star. Infrared sources associated with the center of the Galaxy have also been used extensively as probes of the diffuse ISM, although previous studies suggested (see, e.g., McFadzean et al. 1989) that some of the extinction arises in material associated with denser clouds. *ISO* observations (Lutz et al. 1996) show unequivocally that there is, indeed, a molecular cloud

¹⁰ The notation VI Cygni No. 12, which still occasionally appears in the literature, became obsolete with the adoption of the current designations for OB associations at the IAU General Assembly in Hamburg, 1964.

component to the extinction in this line of sight; the solid-state spectrum is thus a composite of molecular cloud and diffuse ISM features.

2. OBSERVATIONS

Observations were made with the *ISO* short-wavelength spectrometer (SWS). Spectra covering the full SWS range of 2.4–45 μm were taken in low-resolution mode (AOT S01; see de Graauw et al. 1996a for a detailed description of the instrument, its specifications, and its mode of operation). Cyg OB2 No. 12 was first observed on 1995 December 23 (during the commissioning phase of *ISO*) at scan speed 1 (resolving power $R = \lambda/\Delta\lambda = R_0/8$, where $R_0 \approx 1500$ is the full resolving power of the grating, averaged over all wavelengths). A second spectrum was obtained on 1996 October 17 at higher resolution (scan speed 3; $R = R_0/4$). Integration times were approximately 900 s and 3600 s, respectively.

The data were analyzed using the SWS Interactive Analysis package (de Graauw et al. 1996a). Wavelength calibration (Valentijn et al. 1996) is good to an accuracy of 0.01%. The Relative Spectral Response Function (RSRF) of the SWS (see Schaeidt et al. 1996) contains broad structures that might mimic real solid-state features if not correctly removed by the reduction procedure; we compared our data carefully with the RSRF to ensure that no such spurious features are present in the final spectra. Flux calibration (Schaeidt et al. 1996) was checked with reference to ground-based observations from Gezari et al. (1993). The signal-to-noise ratio is excellent at the shortest wavelengths covered by the SWS; however, as the spectrum declines steeply in intensity with increasing wavelength, data at long wavelengths (9–45 μm) are of relatively poor quality and are not discussed further.

Figure 1 combines 2.4–9.0 μm SWS data with the best available ground-based observations in the 7.5–13 μm atmospheric window, the latter taken with the cooled-grating spectrometer CGS3 on the United Kingdom Infrared Telescope at a resolving power $R \approx 50$ (Bowey, Adamson, & Whittet 1997). The CGS3 fluxes were scaled by a constant factor chosen to best match the SWS data in the region of overlap. Broadband fluxes deduced from mean

ground-based photometry (Gezari et al. 1993) are also plotted.

SWS observations of the Galactic center source Sgr A* reported elsewhere (Lutz et al. 1996) are used here as a comparison to our spectrum of Cyg OB2 No. 12. These observations were taken in the same mode (AOT S01) at speed 4 (resolving power $R_0/2$). Of the sources studied by McFadzean et al. (1989), the SWS beam included IRS 3, IRS 7, and IRS 12, but excluded IRS 19.

3. CYGNUS OB2 NO. 12

3.1. Overview

As a member of the Cyg OB2 association, at a distance of 1.7 ± 0.2 kpc (Torres-Dodgen, Tapia, & Carroll 1991), star No. 12 is among the most luminous in the Galaxy; Humphreys (1978) deduced spectral type B5 Ia⁺, absolute magnitude $M_V = -9.9$, and visual extinction $A_V = 10.2 \pm 0.3$ mag. It is significantly more reddened than other members of the association; this might be interpreted as evidence for excess extinction arising in a dusty circumstellar shell or disk (Reddish 1967), but this possibility appears to be ruled out by the absence of dust emission (Persi & Ferrari-Toniolo 1982). The spectral energy distribution (Fig. 1) shows a steeply falling continuum beyond 2.5 μm , consistent with a stellar photosphere modified by the effects of reddening and stellar wind (Leitherer et al. 1984). More likely, the unusually high degree of extinction arises because of an uneven spatial distribution of intracluster material within the Cyg OB2 association (see McMillan & Tapia 1977, who adopt a two-slab model to explain observations of linear and circular polarization). Irrespective of its location, the optical properties of the dust appear to be typical of the diffuse ISM: the ratio of total-to-selective extinction ($R_V = A_V/E_{B-V} = 2.90 \pm 0.15$; Adamson, Whittet, & Duley 1990) and the wavelength of maximum polarization ($\lambda_{\text{max}} = 0.49 \pm 0.01$ μm ; McMillan & Tapia 1977) are well within the normal range (if somewhat below average), consistent with an absence of the growth processes that occur in dense molecular clouds.

Silicate absorption near 10 μm in Cyg OB2 No. 12 was first reported by Rieke (1974). Its peak optical depth in our combined spectrum (Fig. 1) is $\tau_{9.7} = 0.54 \pm 0.06$, consistent with previous estimates (Gillett et al. 1975; Roche & Aitken 1984). (The SWS data alone give essentially the same result with greater uncertainty.) Its profile matches that of circumstellar silicate emission in the red supergiant μ Cephei and is narrower than that observed in molecular clouds (Roche & Aitken 1984; Bowey et al. 1997); this suggests structural and compositional similarity between diffuse ISM dust and “stardust” ejected by evolved stars. Apart from the silicate feature, there is a general absence of prominent ($\tau \gtrsim 0.1$) absorption features in Figure 1. However, the possibility of detecting (or setting limits on) weaker features that might represent abundant, previously hidden components of the dust is important as a means of further constraining dust composition in the diffuse ISM.

3.2. Hydrated Silicates

Our spectra show convincing evidence for a broad, shallow absorption feature centered at 2.75 μm (Fig. 2). This feature is also discernible in an earlier spectrum obtained with the Kuiper Airborne Observatory (KAO) by Knacke et al. (1985), although these authors regarded it as a marginal detection because of problems with cancellation of tellu-

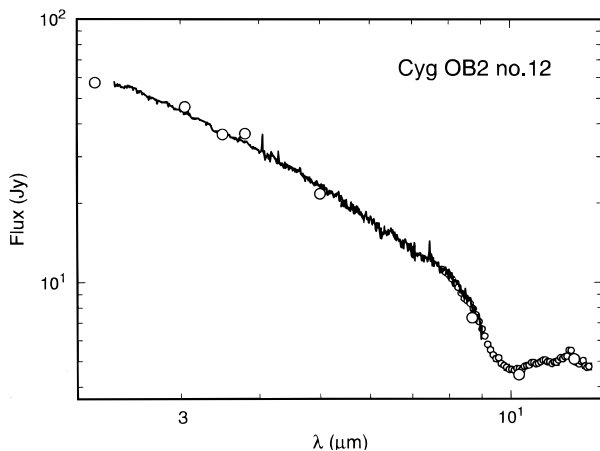


FIG. 1.—Spectral energy distribution of Cyg OB2 No. 12 from 2.2 to 13.5 μm . Continuous curve: *ISO* SWS (speed 3) spectrum. Small open circles: ground-based spectrum in the 10 μm window from Bowey et al. (1997). Large open circles: mean ground-based photometry from the compilation of Gezari et al. (1993). Peaks at 4.05 and 7.46 μm are stellar H (Br α and Pf α) emission lines.

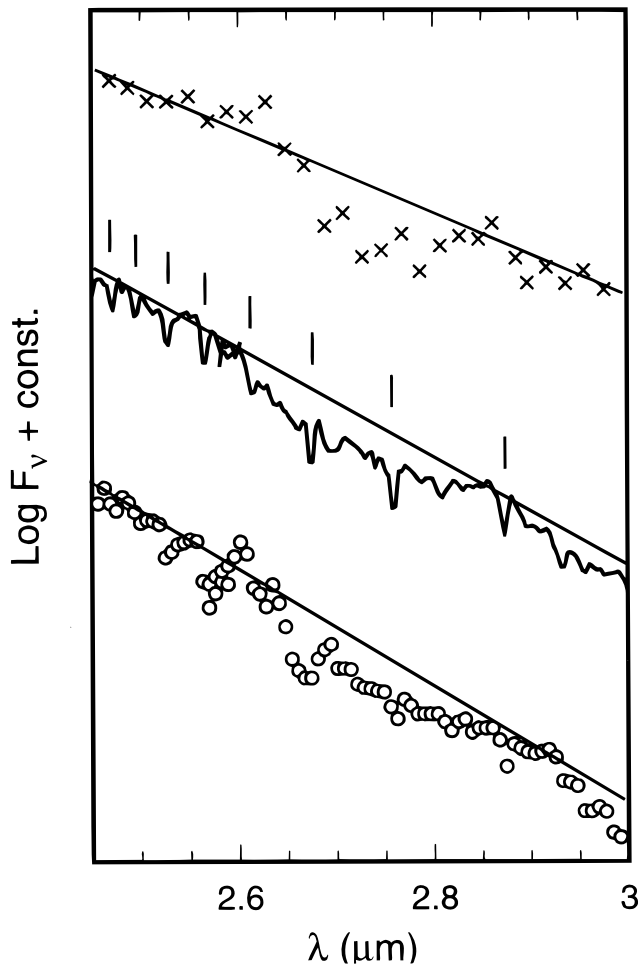


FIG. 2.—Comparison of KAO and ISO spectra of Cyg OB2 No. 12 in the range 2.4–3.0 μm . The KAO data (*crosses, above*) are from Knacke et al. (1985) and have resolving power $R \approx 80$. The ISO data have $R \approx 400$ (SWS speed 3, *continuous curve, center*) and $R \sim 200$ (SWS speed 1, *open circles, below*). Estimated continua for the 2.75 μm feature are shown. Narrow features apparent in the central spectrum arise from stellar H absorption (Pfund series 11–18, marked by vertical lines).

ric features. SWS and KAO spectra are compared in Figure 2. The peak optical depth in the higher quality SWS spectrum is $\tau_{2.75} = 0.035 \pm 0.010$, and the width is $\sim 0.15 \mu\text{m}$ (FWHM). Spectral features in the 2.7–3.2 μm region are characteristic of O–H stretching modes in OH groups or H_2O molecules. Given the absence of ice along the line of sight to Cyg OB2 No. 12 (see § 3.3), we ascribe the 2.75 μm feature to OH groups in interstellar phyllosilicates.¹¹

Phyllosilicates (or layer-lattice silicates) commonly consist of planar silicon-oxygen networks that contain OH groups in the center of a hexagonal arrangement of SiO_4 tetrahedra (Hurlbut & Klein 1977). Three divalent (Mg, Fe^{2+}) or two trivalent (Al^{3+} , Fe^{3+}) ions in a hydroxide structure are coordinated to these sheets through two O atoms and the OH group. These layer units in the crystal can be linked to each other through weak van der Waals forces (as in talc), interlayer cations (mica), H bonding between OH groups and O atoms (serpentine), or through interleaved MgFeAl hydroxides (chlorites). Finally, sheets

¹¹ A similar feature observed in SN 1987A (Timmermann & Larson 1993) was also attributed to OH resonances in silicates; however, this identification must be treated with caution in view of the lack of convincing evidence for a corresponding 9.7 μm silicate feature in SN 1987A.

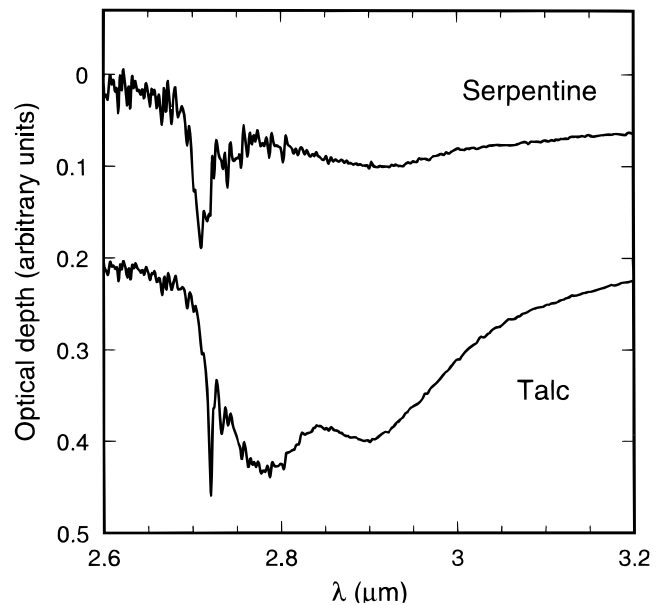


FIG. 3.—Laboratory 2.6–3.2 μm transmittance spectra of serpentine and talc, obtained by T. J. Wdowiak (1997, private communication). Sharp features in the 2.70–2.75 μm region are caused by isolated OH groups, and broader features in the 2.75–3.2 μm region are caused by interlayered H_2O molecules (see § 3.2).

of water molecules can be interlayered between these silicate structures (giving clays their water swelling properties). The position, width, and strength of the OH stretching vibration in terrestrial phyllosilicates depends on the composition and structure of the mineral (see Farmer 1974 for a comprehensive review). The infrared spectra of phyllosilicates in an astrophysical context have been discussed by, among others, Knacke et al. (1985), Wada, Sakata, & Tokunaga (1991), and Tielens et al. (1996).¹²

Sample laboratory spectra of talc ($\text{Mg}_3\text{Si}_4\text{O}_{10}[\text{OH}]_2$) and serpentine ($\text{Mg}_3\text{Si}_2\text{O}_5[\text{OH}]_4$) are shown in Figure 3 (T. J. Wdowiak 1997, private communication). These spectra are characterized by sharp features in the 2.70–2.75 μm region caused by isolated OH groups, and broader features in the 2.75–3.2 μm region caused by interlayered H_2O molecules. The precise position and width of the feature arising in OH groups is dependent on the cation involved and the form of bonding. In talc, for example, it is very narrow ($\sim 0.003 \mu\text{m}$), but disordered structure and superposition of bands caused by the presence of more than one cation produces features typically a factor of 10 broader, as is the case for serpentine. Other phyllosilicates, notably chlorites ($[\text{Mg}, \text{Fe}, \text{Al}]_{12}[\text{Si}, \text{Al}]_8\text{O}_{20}[\text{OH}]_{16}$), with their interleaved hydroxides, have yet broader features because of the presence of more than one type of OH group. The peak position of the observed 2.75 μm feature is close to that of isolated OH groups in talcs or serpentines, but the observed feature is much broader than is characteristic for such minerals (0.15 μm compared with 0.03 μm). Chlorites provide better agreement in terms of width, but Mg/Fe chlorites absorb at longer wavelengths (2.85 μm ; Farmer 1974, especially p. 331; Knacke et al. 1985). Another possibility is Al cation-dominated chlorites, which absorb at $\sim 2.75 \mu\text{m}$.

¹² Note that the spectrum labeled “talc” shown by Tielens et al. (1996, their Fig. 3) is dominated by water of hydration, and that that mineral should more properly have been called vermiculite, the hydrated form of talc.

Unfortunately, the weakness of the observed feature in the spectrum of Cyg OB2 No. 12 does not permit a detailed comparison with laboratory spectra.

The peak strength of the OH feature in typical phyllosilicates is $\sim 2 \times 10^{-19}$ cm² molecule⁻¹ (Rossman 1988), from which we estimate a column density $N(\text{OH}) \sim 2 \times 10^{17}$ cm⁻² toward Cyg OB2 No. 12. This represents $\sim 1\%$ of the solar O abundance [assuming $N(\text{H}) \approx 2 \times 10^{21} A_V \approx 2 \times 10^{22}$ cm⁻²]. In contrast, essentially all of the available Si is tied up in silicates. It follows that silicates in the diffuse ISM toward Cyg OB2 No. 12 contain only a few percent by mass of OH. This is consistent with the expected OH fraction in terrestrial minerals such as serpentine and talc. However, only a small fraction of interstellar silicates might be hydrated, so this does not rule out forms with higher degrees of hydration, such as chlorites.

In summary, we conclude that the width of the interstellar 2.75 μm feature points toward OH bonded to a large number of different cations in a number of different environments, likely including interleaved hydroxides in a chlorite structure. Our detection implies that at least one component of interstellar silicate dust forms under conditions that favor hydration. A possible source might be surface reactions between silicate grains and gaseous H₂O in the outflows of red giants. However, thermodynamic calculations suggest that this reaction will occur at around 350 K (Grossman & Larimer 1974), and at such low temperatures it is likely to be kinetically inhibited in the short expansion timescales of such outflows (Prinn & Fegley 1987).¹³ Hydration of silicates in the ISM itself is highly implausible under typical conditions because of the low equilibrium dust temperature. A possible route might involve inward diffusion of adsorbed H atoms, which is possible even at interstellar temperatures; localized, transient heating events associated with cosmic-ray hits might then conceivably lead to the structural rearrangement required to form a hydrated silicate. Likewise, an H₂O ice layer accreted inside a dense cloud might also react rapidly with a silicate grain at a hot spot produced by a cosmic ray impact.

3.3. Ices and Organics

The 2.85–3.75 μm region of our highest resolution SWS spectrum of Cyg OB2 No. 12 is illustrated in Figure 4. This spectral region contains the wavelengths of O–H stretching resonances in water ice and the C–H stretching resonances in carbon-bearing ices and organic molecules. A weak structure appears in the O–H stretch region, but this does not resemble either water ice or silicate hydration. The weak feature at 3.15 μm appears to be real but does not correspond to any known or expected resonance in interstellar dust. We deduce a limiting optical depth of $\tau_{3.05} \lesssim 0.02$ on the strength of absorption due to water ice, consistent with previous ground-based and airborne observations (Gillett et al. 1975; Knacke et al. 1985). Assuming an integrated band strength of 2×10^{-16} cm molecule⁻¹ for water ice (Gerakines et al. 1995) and width 350 cm⁻¹, we deduce $N(\text{H}_2\text{O}) \lesssim 4 \times 10^{16}$ cm⁻² in ices. The abundance of O in H₂O ice in this line of sight is thus no more than 2×10^{-6} , or 0.2% of the solar abundance. Similarly, our spectra show no discernible absorption at the position of the strong 4.27

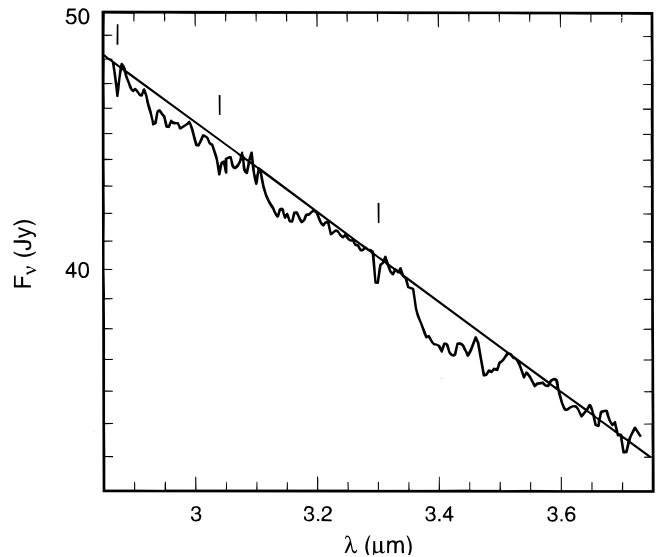


FIG. 4.—SWS spectrum of Cyg OB2 No. 12 in the range 2.85–3.75 μm at resolving power ≈ 400 . The estimated continuum for the 3.4 μm “hydrocarbon” feature is shown. Narrow features at 3.30, 3.04, and 2.87 μm arise from stellar H absorption (Pfd, Pfc, and Pfl1, marked by vertical lines).

μm resonance of CO₂ (Fig. 5). We estimate a limit of $\tau_{4.27} \lesssim 0.02$, and hence $N(\text{CO}_2) \lesssim 5 \times 10^{15}$ cm⁻², assuming a band strength of 7.6×10^{-17} cm molecule⁻¹ (Gerakines et al. 1995) and width 20 cm⁻¹. This nondetection of CO₂ ice is consistent with the upper limit for the H₂O ice column density, as CO₂ appears to be present at $\sim 15\%$ of the H₂O abundance in lines of sight that pass through molecular clouds (de Graauw et al. 1996b).

The most prominent absorption in Figure 4 is the 3.4 μm feature attributed to the CH₂ and CH₃ stretching modes in aliphatic hydrocarbons (Adamson et al. 1990; Sandford et al. 1991; Pendleton et al. 1994). Its peak optical depth in our spectrum ($\tau_{3.4} = 0.04 \pm 0.01$) is consistent with ground-

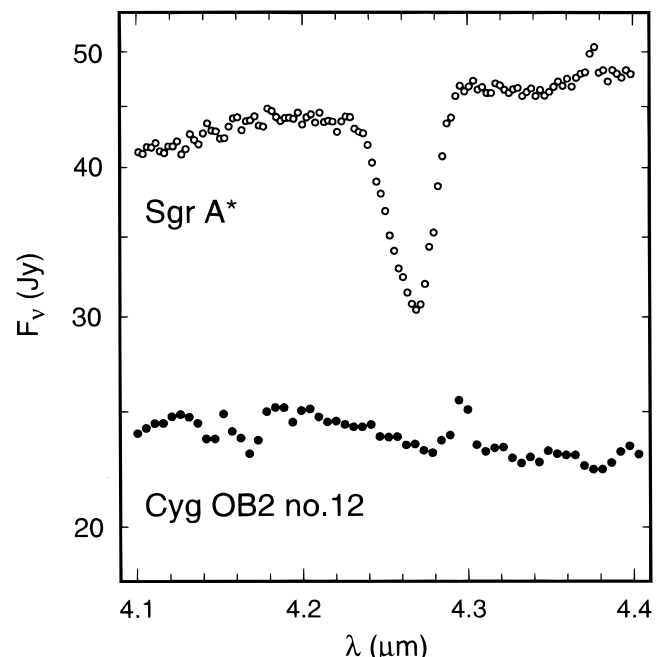


FIG. 5.—Comparison of SWS spectra of Sgr A* (open circles) and Cyg OB2 No. 12 (filled circles) in the region of the 4.27 μm feature of CO₂. The Sgr A* data have been displaced upward by 15 Jy for display.

¹³ Hydrated silicates in solar system meteorites are formed through aqueous alteration on a planetary body (Zolensky & McSween 1988).

based measurements. Assuming a band strength 5×10^{-18} cm per C atom (Sandford et al. 1991), this translates to $\sim 5\%$ of the solar abundance of C in C—H bonds. The subfeature at $3.48 \mu\text{m}$ is quite prominent and appears somewhat deeper (relative to the main $3.4 \mu\text{m}$ feature) in our spectrum compared with ground-based observations of Cyg OB2 No. 12 and other lines of sight (see, e.g., Pendleton et al. 1994).

We searched our spectra for additional absorption features attributable to dust at longer wavelengths. A weak feature at $\sim 6.2 \mu\text{m}$ ($\tau_{6.2} = 0.06 \pm 0.04$) is attributed to C=C stretching modes in aromatic hydrocarbons (see Schutte et al. 1997 for detailed discussion), but no other features deeper than $\tau \sim 0.04$ are discernible in the $4\text{--}8 \mu\text{m}$ range. There is no convincing evidence for features associated with C≡N or carbonyl (C=O) molecular groups near 4.6 and $5.6 \mu\text{m}$, respectively, or for CH₂ and CH₃ deformation modes near $6.8 \mu\text{m}$.

4. COMPARISON WITH SAGITTARIUS A*

Unlike Cyg OB2 No. 12, sources associated with the Galactic center show absorptions at $2.8\text{--}3.2$ and $5.8\text{--}6.2 \mu\text{m}$ associated with OH stretching and bending modes (McFadzean et al. 1989; Tielens et al. 1996). Analysis of $3 \mu\text{m}$ spectra led McFadzean et al. to argue that the total extinction to the Galactic center has two components: a spatially variable molecular cloud component producing $3.0 \mu\text{m}$ ice absorption and a constant diffuse cloud component producing $3.4 \mu\text{m}$ absorption due to hydrocarbons. The case for relatively dense molecular material is supported by gas phase CO $J = 3\text{--}2$ observations (Sutton et al. 1990), which indicate the presence of at least three absorptions attributed to foreground molecular clouds with distinct radial velocities in the line of sight to Sgr A* ($v_{\text{LSR}} \approx -53, -31, \text{ and } -3 \text{ km s}^{-1}$). The first of these is part of the 3 kpc spiral arm, the second a large-scale inner Galactic feature, and the last probably local to the solar neighborhood (see Geballe, Baas, & Wade 1989 and references therein). Observations of NH₃ indicate temperatures for these clouds in the range $14\text{--}19 \text{ K}$ (Serabyn & Güsten 1986), consistent with the presence of ice mantles on grains. The implied gas-phase CO column density (summed over all three clouds) is $N(\text{CO}) \sim 5 \times 10^{17} \text{ cm}^{-2}$, which suggests a total extinction of $A_V \sim 5\text{--}10$ mag in molecular clouds if they have similar properties to the Taurus dark cloud in the solar neighborhood (see Whittet & Duley 1991).

Detection of solid CO₂ absorption toward Sgr A* (Lutz et al. 1996; de Graauw et al. 1996b) provides strong confirmation of the presence of ices along the line of sight and leads to the conclusion that the 3.0 and $6.0 \mu\text{m}$ features are primarily caused by H₂O ice in molecular clouds. Figure 5 illustrates the striking contrast between Sgr A* and Cyg OB2 No. 12 in the CO₂ stretch region. Both stretching and bending modes of CO₂ are detected in Sgr A* (Lutz et al. 1996) with optical depths $\tau_{4.27} = 0.72 \pm 0.04$ and $\tau_{15.2} = 0.07 \pm 0.02$, consistent with a column density $N(\text{CO}_2) \approx 1.5 \times 10^{17} \text{ cm}^{-2}$ (de Graauw et al. 1996b). This may be compared with $N(\text{H}_2\text{O}) \approx 1.2 \times 10^{18} \text{ cm}^{-2}$, deduced from the $3.0 \mu\text{m}$ feature. The CO₂/H₂O ice ratio is thus $\sim 13\%$, similar to that in other lines of sight that pass through molecular clouds (de Graauw et al. 1996b). Chiar et al. (1995) find a reasonably close correlation between $N(\text{H}_2\text{O})$ and A_V (see their Fig. 4) in molecular clouds in the solar neighborhood. If this correlation also holds toward Sgr A*,

extinction in the range $10 < A_V < 15$ mag would be consistent with the observed value of $N(\text{H}_2\text{O})$. Thus, $[A_V]_{\text{MC}} \sim 10$ mag in molecular clouds is compatible with both the gas phase CO column density (above) and the depth of the ice feature. Comparing this value with the total extinction ($A_V \approx 30$ mag; see, e.g., McFadzean et al. 1989), we estimate that $[A_V]_{\text{DISM}} \sim 20$ mag arises in the diffuse ISM toward Sgr A* (compared with ~ 10 mag toward Cyg OB2 No. 12).

The $2.6\text{--}3.3 \mu\text{m}$ region of the SWS spectrum of Sgr A* is dominated by the broad $3.0 \mu\text{m}$ ice feature ($\tau_{3.0} \approx 0.65$), and this presents a serious hindrance to detection of silicate hydration features in this line of sight. A weak $2.75 \mu\text{m}$ feature comparable in strength to that in Cyg OB2 No. 12 would be very difficult to detect, but a feature of depth $\tau_{2.75} \sim 0.2$ (predicted if Sgr A* has the same $\tau_{2.75}/\tau_{9.7}$ ratio as Cyg OB2 No. 12) can be excluded. It may therefore be the case that silicates toward Sgr A* contain less structural OH than those toward Cyg OB2 No. 12. The possibility that silicates toward the Galactic center contain significant quantities of interlayered water of hydration contributing to the observed $3.0 \mu\text{m}$ feature (Tielens et al. 1996) can probably be excluded, as thermal processing tends to remove H₂O more readily than bonded OH ions (Timmermann & Larson 1993).

Like Cyg OB2 No. 12, the Galactic center shows absorptions at 3.4 and $6.2 \mu\text{m}$ attributed to aliphatic and aromatic hydrocarbons, respectively, in the diffuse ISM (Sandford et al. 1991; Lutz et al. 1996; Schutte et al. 1997). Unlike Cyg OB2 No. 12, the Sgr A* spectrum also contains an absorption feature at $6.8 \mu\text{m}$, attributed to CH₂ and CH₃ deformation modes, which is likely a superposition of absorptions arising in the diffuse ISM and molecular clouds. The non-detection of the $6.8 \mu\text{m}$ feature in Cyg OB2 No. 12 is not surprising, given the comparative weakness of the C—H stretching mode and the absence of molecular cloud material in this line of sight.

5. IMPLICATIONS FOR DUST COMPOSITION

The observed infrared features allow quantitative estimates of the contributions the carriers make to the total grain mass or volume (Tielens & Allamandola 1987). Using our spectrum of Cyg OB2 No. 12, we followed a procedure identical to that applied by Tielens et al. (1996) to observations of the Galactic center. The volume per hydrogen atom occupied by a grain material of bulk density $\rho(X)$, molecular mass $m(X)$, and column density $N(X)$ is

$$V(X) = \frac{1}{\rho(X)} \frac{N(X)}{N(\text{H})} m(X).$$

For silicates, we assume a density of 2.5 g cm^{-3} , composition (Mg, Fe)SiO₄, and band strength $2 \times 10^{-16} \text{ cm (Si atom)}^{-1}$ for the $9.7 \mu\text{m}$ feature; similarly, for aliphatic hydrocarbons, we assume a density of 1 g cm^{-3} , composition —CH₃, and $3.4 \mu\text{m}$ band strength $5 \times 10^{-18} \text{ cm (C atom)}^{-1}$. We thus calculate $V(\text{silicate}) \approx 3.9 \times 10^{-27} \text{ cm}^3 (\text{H atom})^{-1}$ and $V(\text{hydrocarbon}) \approx 0.3 \times 10^{-27} \text{ cm}^3 (\text{H atom})^{-1}$ from the observed features¹⁴ toward Cyg OB2 No. 12. These values may be compared with the expected total grain volume, deduced by Kramers-Krönig

¹⁴ We have not attempted to include the carrier of the $6.2 \mu\text{m}$ C=C feature in these calculations, in view of both the relatively large uncertainty in the strength of the observed feature and the large range in possible band strengths for aromatic carbonaceous solids (see Schutte et al. 1997).

analysis of the interstellar extinction curve to be $V(\text{total}) \approx 7 \times 10^{-27} \text{ cm}^3 (\text{H atom})^{-1}$ (Spitzer 1978; Tielens & Allamandola 1987; Tielens et al. 1996). Thus, silicates toward Cyg OB2 No. 12 may contribute ~50%–60% of the total grain volume, but hydrocarbons responsible for the 3.4 μm feature contribute only ~4%. Tielens et al. (1996) estimate a similar contribution from silicates (~60%) and a somewhat larger contribution from aliphatic hydrocarbons (~10%) toward the Galactic center.

These calculations are subject to considerable uncertainty, particularly in the assumed band strengths, and should be treated with caution. Nevertheless, it is well known (see, e.g., Gillett et al. 1975) that silicates alone cannot account for the visible extinction, as they produce insufficient A_V per unit 9.7 μm opacity. Small ($<0.03 \mu\text{m}$) graphitic grains are widely assumed to account for the 0.217 μm “extinction bump” in the ultraviolet but contribute negligible extinction in the visible. If the balance of the visible extinction is made up by carbonaceous solids in larger grains, then much of this material seems likely to be in an aromatic form, such as amorphous carbon, in addition to aliphatics responsible for the 3.4 μm feature. C=C stretching modes in aromatic solids are relatively weak, such that, in principle, large fractions of the available

carbon might, indeed, be tied up in the component of the dust responsible for the 6.2 μm feature (see Schutte et al. 1997). It should be remembered that these and other carbonaceous solids are subject to stringent limits on the total interstellar abundance of elemental C (Mathis 1996). Taking all these factors into account, a reasonable model for the composition of dust toward Cyg OB2 No. 12 based on existing infrared spectroscopy is silicate:carbon in the volume ratio ~3:2, the carbonaceous component being predominantly aromatic.

As silicates account for virtually all of the available Si and Mg atoms in the ISM, the best possibility for a further oxygen-rich grain component of significant abundance would appear to be oxides of iron (see, e.g., Jones 1990). The latter absorb near 20 μm (close to the silicate bending mode) and a detailed examination of this spectral region will be an important future goal.

We are grateful to Tom Wdowiak for providing us with unpublished spectra of talc and serpentine and to Andy Adamson for comments on the text. D. C. B. W. is funded by NASA grants NAGW-3144 and NAGW-4039. The ISO research of E. F. v.D. and W. S. is supported by ASTRON and SRON.

REFERENCES

- Adamson, A. J., Whittet, D. C. B., & Duley, W. W. 1990, *MNRAS*, 243, 400
 Bowey, J. E., Adamson, A. J., & Whittet, D. C. B. 1997, *MNRAS*, submitted
 Chiar, J. E., Adamson, A. J., Kerr, T. H., & Whittet, D. C. B. 1995, *ApJ*, 455, 234
 de Graauw, Th., et al. 1996a, *A&A*, 315, L49
 ———. 1996b, *A&A*, 315, L345
 Farmer, V. C. 1974, *The Infrared Spectra of Minerals* (London: Mineralogical Society)
 Geballe, T. R., Baas, F., & Wade, R. 1989, *A&A*, 208, 255
 Gerakines, P. A., Schutte, W. A., Greenberg, J. M., & van Dishoeck, E. F. 1995, *A&A*, 296, 810
 Gezari, D. Y., Schmitz, M., Pitts, P. S., & Mead, J. M. 1993, *Catalog of Infrared Observations*, NASA Ref. Publ. 1294 (Washington, DC: NASA)
 Gillett, F. C., Jones, T. W., Merrill, K. M., & Stein, W. A. 1975, *A&A*, 45, 77
 Grossman, L., & Larimer, J. W. 1974, *Rev. Geophys. Space Phys.*, 12, 71
 Humphreys, R. M. 1978, *ApJS*, 38, 309
 Hurlbut, C. S., & Klein, C. 1977, *Manual of Mineralogy* (New York: Wiley & Sons)
 Jones, A. P. 1990, *MNRAS*, 245, 331
 Jones, A. P., Tielens, A. G. G. M., Hollenbach, D. J., & McKee, C. F. 1994, *ApJ*, 433, 797
 Knacke, R. F., Puetter, R. C., Erickson, E., & McCorkle S. 1985, *AJ*, 90, 1828
 Leitherer, C., Bertout, C., Stahl, O., & Wolf, O. 1984, *A&A*, 140, 199
 Lutz, D., et al. 1996, *A&A*, 315, L269
 Mathis, J. S. 1990, *ARAA*, 28, 37
 ———. 1996, *ApJ*, 472, 643
 McFadzean, A. D., Whittet, D. C. B., Longmore, A. J., Bode, M. F., & Adamson, A. J. 1989, *MNRAS*, 241, 873
 McMillan, R. S., & Tapia, S. 1977, *ApJ*, 212, 714
 Pendleton, Y. J., Sandford, S. A., Allamandola, L. J., Tielens, A. G. G. M., & Sellgren, K. 1994, *ApJ*, 437, 683
 Persi, P., & Ferrari-Toniolo, M. 1982, *A&A*, 111, L7
 Prinn, R. G., & Fegley, B. J. 1987, *Annu. Rev. Earth Planet. Sci.*, 15, 171
 Reddish, V. 1967, *MNRAS*, 135, 251
 Rieke, G. H. 1974, *ApJ*, 193, L81
 Roche, P. F., & Aitken, D. K. 1984, *MNRAS*, 208, 481
 Rossman, G. R. 1988, *Rev. Mineralogy*, 18, 193
 Sandford, S. A., Allamandola, L. J., Tielens, A. G. G. M., Sellgren, K., Tapia, M., & Pendleton, Y. J. 1991, *ApJ*, 371, 607
 Schaeidt, S. G., et al. 1996, *A&A*, 315, L55
 Schutte, W. A., et al. 1997, *A&A*, submitted
 Serabyn, E., & Güsten, R. 1986, *A&A*, 161, 334
 Spitzer, L. 1978, *Physical Processes in the Interstellar Medium* (New York: Wiley & Sons)
 Sutton, E. C., Danchi, W. C., Jaminet, P. A., & Masson, C. R. 1990, *ApJ*, 348, 503
 Tielens, A. G. G. M., & Allamandola, L. J. 1987, in *Interstellar Processes*, ed. D. J. Hollenbach & H. A. Thronson (Dordrecht: Reidel), 397
 Tielens, A. G. G. M., Wooden, D. H., Allamandola, L. J., Bregman, J., & Witteborn, F. C. 1996, *ApJ*, 461, 210
 Timmermann, R., & Larson, H. P. 1993, *ApJ*, 415, 820
 Torres-Dodgen, A. V., Tapia, M., & Carroll, M. 1991, *MNRAS*, 249, 1
 Valentijn, E. A., et al. 1996, *A&A*, 315, L60
 Wada, S., Sakata, A., & Tokunaga, A. T. 1991, *ApJ*, 375, L17
 Whittet, D. C. B., & Duley, W. W. 1991, *A&A Rev.*, 2, 167
 Whittet, D. C. B., Duley, W. W., & Martin, P. G. 1990, *MNRAS*, 244, 427
 Zolensky, M., & McSween, H. Y. 1988, in *Meteorites and the Early Solar System*, ed. J. F. Kerridge & M. Mathews (Tucson: Univ. Arizona Press), 114